Photonic crystal circular-shaped microcavity and its uniform cavity-waveguide coupling property due to presence of whispering gallery mode

Po-Tsung Lee, Tsan-Wen Lu*, Chia-Ming Yu, and Chung-Chuan Tseng

Department of Photonics and Institute of Electro-Optical Engineering, National Chiao Tung University
Rm. 415, CPT Building, 1001 Ta Hsueh Road, 300 Hsinchu, Taiwan, R.O.C.
ricky.eo94g@nctu.edu.tw

Abstract: In this report, we investigate a photonic crystal circular-shaped microcavity (removing seven air holes) sustaining whispering-gallery mode (WGM) by shifting the 12 nearest air holes according to the concept of cavity-shaping in micro-disk and micro-gear lasers. The WGM modal characteristics are investigated by three-dimensional (3D) finite-difference time-domain (FDTD) simulations. From well-fabricated devices and simulated results, we obtain and identify WGM single-mode lasing with low threshold and high measured quality factor. By inserting additional waveguides, we also investigate its uniform coupling behaviors in different waveguide-cavity-waveguide geometries in both FDTD simulations and experiments.

OCIS codes: (050.5298) Photonic crystals; (140.5960) Semiconductor lasers; (140.3945) Microcavities

References and links

1. A. Yariv, Y. Xu, R. K. Lee, and A. Scherer, "Coupled-resonator optical waveguide: a proposal and analysis," Opt. Lett. **24**, 711-713 (1999).
2. S. J. Choi, Z. Peng, Q. Yang, S. J. Choi, and P. D. Dapkus, "Eight-channel microdisk CW laser arrays vertically coupled to common output bus waveguides," IEEE Photon. Technol. Lett. **16**, 356-358 (2004).
3. S. Ishii, A. Nakagawa, and T. Baba, "Modal Characteristics and Bistability in Twin Microdisk Photonic Molecule Lasers," IEEE J. Sel. Top. Quantum Electron. **12**, 71-77 (2006).
4. O. Painter, R. K. Lee, A. Scherer, A. Yariv, J. D. O'Brien, P. D. Dapkus, and I. Kim, "Two-dimensional photonic band-gap defect mode laser," Science **284**, 1819-1821 (1999).
5. Y. Akahane, T. Asano, B. S. Song, and S. Noda, "High-Q photonic nanocavity in a two-dimensional photonic crystal," Nature (London) **425**, 944-947 (2003).
6. H. Y. Ryu, H. G. Park, and Y. H. Lee, "Two-dimensional Photonic Crystal Semiconductor Lasers: Computational Design, Fabrication, and Characterization," IEEE J. Sel. Top. Quantum Electron. **8**, 891-908 (2002).
7. K. Nozaki and T. Baba, "Quasiperiodic photonic crystal microcavity lasers," Appl. Phys. Lett. **84**, 4875-4877 (2004).
8. D. Chang, J. Scheuer, and A. Yariv, "Optimization of circular photonic crystal cavities: beyond coupled mode theory," Opt. Express **13**, 9272-9279 (2005).
9. P. T. Lee, T. W. Lu, F. M. Tsai, T. C. Lu, and H. C. Kuo, "Whispering gallery mode of modified octagonal quasiperiodic photonic crystal single-defect microcavity and its side-mode reduction," Appl. Phys. Lett. **88**, 201104 (2006).
10. P. T. Lee, T. W. Lu, F. M. Tsai, and T. C. Lu, "Investigation of whispering-gallery mode dependence on cavity geometry in quasiperiodic photonic crystal microcavity lasers," Appl. Phys. Lett. **89**, 231111 (2006).
11. H. Y. Ryu, M. Notomi, G. H. Kim, and Y. H. Lee, "High quality-factor whispering-gallery mode in the photonic crystal hexagonal disk cavity," Opt. Express **12**, 1708-1719 (2004).
12. M. Fujita and T. Baba, "Microgear laser," Appl. Phys. Lett. **80**, 2051-2053 (2002).
13. K. P. Huy, A Morand, and P. Benech, "Modelization of the whispering gallery mode in microgear resonators using the Floquet-Bloch formalism," IEEE J. Quantum Electron. **41**, 357-365 (2005).
14. K. Nozaki, A. Nakagawa, D. Sano, and T. Baba, "Ultralow threshold and single-mode lasing in Microgear Lasers and its fusion with Quasi-Periodic Photonic Crystals," IEEE. J. Sel. Top. Quantum Electron. **9**, 1355-1360 (2003).

#83638 - $15.00 USD Received 31 May 2007; revised 12 Jul 2007; accepted 12 Jul 2007; published 16 Jul 2007

15. M. K. Seo, K. Y. Jeong, J. K. Yang, Y. H. Lee, H. G. Park, and S. B. Kim, "Low threshold current single-cell hexapole mode photonic crystal laser," Appl. Phys. Lett. **90**, 171122 (2007).
16. S. G. Johnson, S. Fan, A. Mekis, and J. D. Joannopoulos, "Multipole-cancellation mechanism for high-Q cavities in the absence of a complete photonic band gap," Appl. Phys. Lett. **78**, 3388-3390 (2001).
17. K. Srinivasan, P. E. Barclay, O. Painter, J. Chen, A. Y. Cho, and C. Gmachl, "Experimental demonstration of a high quality factor photonic crystal microcavity," Appl. Phys. Lett. **83**, 1915-1917 (2003).
18. A. Faraon, E. Waks, D. Englund, I. Fushman, and J. Vuckovic, "Efficient photonic crystal cavity-waveguide couplers," Appl. Phys. Lett. **90**, 073102 (2007).
19. I. Park, H. S. Lee, H. J. Kim, K. M. Moon, S. G. Lee, B. H. O, S. G. Park, and E. H. Lee, "Photonic crystal power-splitter based on directional coupling," Opt. Express **12**, 3599-3604 (2004).
20. M. Notomi, A. Shinya, S. Mitsugi, E. Kuramochi, and H. Ryu, "Waveguides, resonators and their coupled elements in photonic crystal slabs," Opt. Express, **12**, 1551 (2004).
21. "G. H. Kim, Y. H. Lee, A. Shinya, and M. Notomi, "Coupling of small, low-loss hexapole mode with photonic crystal slab waveguide," Opt. Express **12**, 6624 (2004).

1. Introduction

Over the past two decades, micro-disk lasers with high quality (*Q*) factor whispering-gallery modes (WGM) have become key components in constructing various optical applications. Because the field distribution of WGM resonance concentrates in the region of cavity-edge, it is very suitable for integration with other optical components by coupling effect in photonic integrated circuits (PICs) on-chip and optical logic applications [1-3]. Unfortunately, the performances of micro-disk lasers, for example, *Q*-factor and threshold, suffer dramatic degradations due to the increasing bend losses when the disk size shrinks to the diffraction limitation. In recent years, the micro and nanocavities formed by photonic crystal (PC) with photonic band gap (PBG) have successfully overcome above performance degradations and show excellent performances including high *Q*-factor and low threshold when minimizing the cavity size [4-6]. However, in most present commonly-used PC cavity designs, WGM is rarely well-sustained or not the only mode able to lase in the designed range. In very recent reports, several groups have investigated and demonstrated WGM lasing in microcavities formed by various qausiperiodic photonic crystal (QPC) lattices [7-10]. Under optical pumping, all of them show WGM single-mode lasing with high *Q*-factors and low thresholds. Unfortunately, this kind of QPC microcavity is difficult to integrate with the present PC-based passive optical system due to its spatial non-periodic lattice structure. Although it is possible to realize photonic integrated circuits by QPC lattice system, many further investigations are still needed. To overcome this difficult situation, one realistic approach is to enhance or well-localize WGM in PC microcavity by some modifications, for example, the air-hole shifting reported by H. Y. Ryu *et al.* [11]. In our previous report [10], we have shown a strong WGM mode dependence on the boundary geometry of 12-fold QPC microcavity (positions of 12 nearest air holes) and this also provide us a design direction to enhance WGM in PC microcavity.

2. Design and simulation

In micro-disk lasers, it is well known that one can split or enhance specific WGM by shaping the cavity, for examples, square, stadium, elliptical, notched micro-disks, and micro-gear (micro-flower) lasers [12, 13]. In micro-gear lasers, the spacing of the gears formed at the edge of micro-disk is designed to be half of WGM lasing wavelength. And the specific WGM with azimuthal lobes that match with the gears will be well sustained and other resonance modes including π-phase shifting mode, WGMs with mismatched azimuthal lobes, and different order WGMs will be weaken. Recently, it has been proposed theoretically that this geometry can be perfectly fused with 12-fold QPCs [14]. In 12-fold QPC D2 (formed by seven missing air holes) microcavity, the gears formed by 12 nearest air holes also show the similar effect as in micro-gear lasers. And we have demonstrated this idea in experiments with

#83638 - $15.00 USD Received 31 May 2007; revised 12 Jul 2007; accepted 12 Jul 2007; published 16 Jul 2007

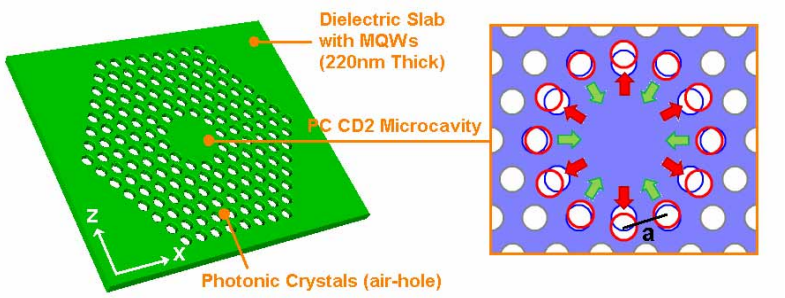

Fig. 1. Scheme and cavity design of PC CD2 microcavity. The PC patterns are defined and fabricated on the dielectric slab consisting of InGaAsP MQWs with thickness of 220nm and refractive index of 3.4. According to the theory in micro-gear lasers, the cavity is modified from PC D2 microcavity to PC CD2 microcavity by shifting the 12 nearest air holes inward or outward to make the spacing between air holes equal to one lattice constant.

high *Q*-factor of 10,000, low threshold of 0.15 mW, and strong WGM mode dependence on the cavity geometry due to this micro-gear effect. As a result, it is possible to sustain a WGM in PC D2 microcavity by shifting the 12 nearest air holes slightly. The scheme of our design is shown in Fig. 1. The PCs are formed by air holes on a thin dielectric slab and the original PC D2 microcavity is formed by removing seven air holes. The positions of 12 nearest air holes are rearranged to form circular boundary geometry with spacing of one lattice constant by moving six of them inward and six of them outward, which is re-named PC circular-D2 (CD2) microcavity due to its cavity shape, as shown in Fig. 1. Actually, this microcavity can be regarded as a micro-gear cavity surrounded by PCs with PBG effect. To confirm this design, we apply three-dimensional (3D) finite-difference time-domain (FDTD) method to simulate the WGM modal characteristics in PC CD2 microcavity. The designed lattice constant (*a*) and the air-hole radius (*r*) over lattice constant ratio (*r/a*) are 500 nm and 0.34. The refractive index of the dielectric material (InGaAsP) is set as 3.4. The simulated electric- and magnetic-

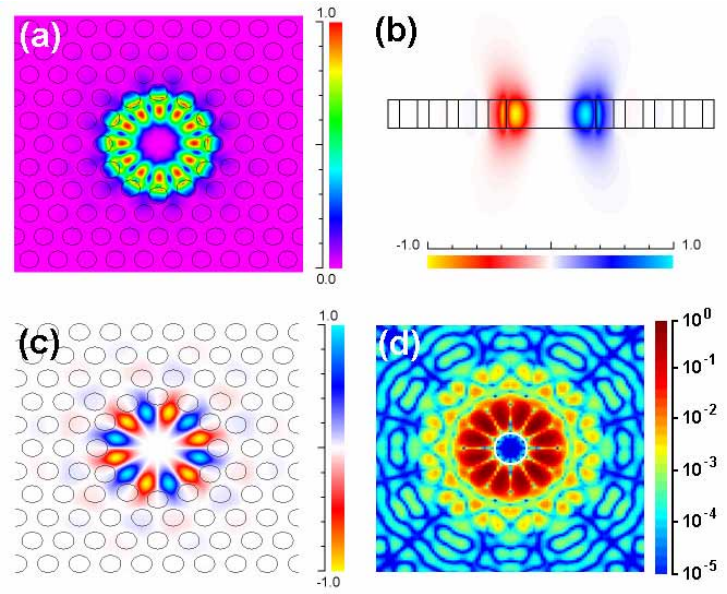

Fig. 2. 3D FDTD simulations of WGM with azimuthal number six. (a) Electric-field distribution in the x-z plane. (b) Electric-field distribution in the x-y plane. (c) Magnetic-field distribution in the x-z plane. (d) WGM electric-field distribution in *k*-space by Fourier transformation.

#83638 - $15.00 USD Received 31 May 2007; revised 12 Jul 2007; accepted 12 Jul 2007; published 16 Jul 2007

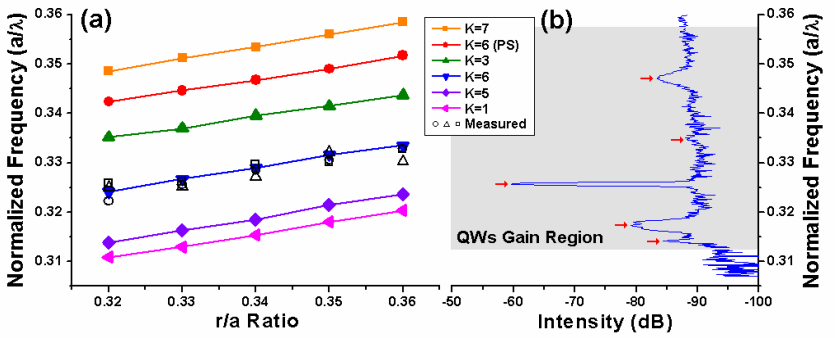

Fig. 3. (a). Plot of normalized frequency versus PC *r/a* ratio of the resonance modes in PC CD2 microcavity by 3D FDTD simulations. The hollow circles, squares, and triangles denote the measured lasing actions from devices with lattice constants from 490 to 510 nm. (b). The measured resonance spectrum from well-fabricated device with lattice constant 500 nm and *r/a* ratio ~ 0.33. We can identify each resonance mode including WGM lasing mode by comparing with the simulated results in (a). The gain region of MQWs is also indicated in the figure.

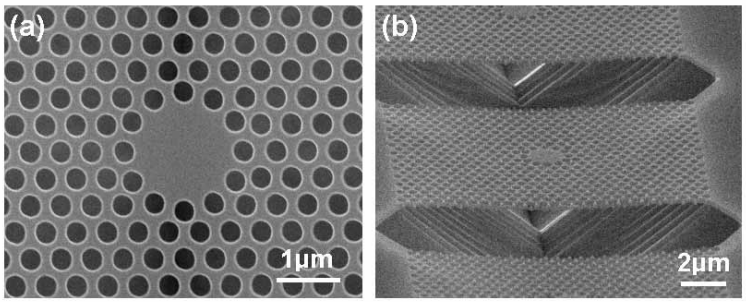

Fig. 4. (a). Top-view and (b) side-view SEM pictures of fabricated PC CD2 microcavity lasers. The fabricated lattice constant and *r/a* ratio are 500 nm and ~0.33.

field distributions of sustained WGM with azimuthal number six whose lobes match with the gears formed by the 12 nearest air holes are shown in Figs. 2(a)-2(c). From the mode distribution in the x-z plane, one can observe a significant zero-distribution region at the center of the microcavity. This indicates that this mode can be severed as a good excited mode for the electrical injection structure by inserting a central post without affecting WGM lasing performance [11, 15]. It is also observed from the electric field in the x-y plane that only a very small fraction of energy radiates into vertical directions due to the modal cancellation [16] of WGM, which implies its high *Q*-factor. This can also be seen from the electric-field distribution in the wave-vector (*k*) space by Fourier transformation, as shown in Fig. 2(d). Only very few leaky components are inside the light cone. We also calculate other resonance modes in PC CD2 microcavity within our designed range including K = 1, 3 (both are classified as first-order WGM) and K = 5, 6, 7 (all are classified as zero-order WGM, including phase-shifting mode, denoted as PS), where K denotes the Bloch number. The plot of normalized frequency of the resonance modes versus PC *r/a* ratio is shown in Fig. 3(a).

3. Fabrication

To demonstrate our proposed design, the real devices are fabricated by a series of well-developed fabrication processes illustrated below. First, the epitaxial structure consisting of four 10 nm compressively-strained InGaAsP multi-quantum-wells (MQWs) on InP substrate as the active layer is grown by metal-organic chemical vapor deposition (MOCVD) system. Its photoluminescence (PL) centered at 1550 nm wavelength under room temperature is

#83638 - $15.00 USD Received 31 May 2007; revised 12 Jul 2007; accepted 12 Jul 2007; published 16 Jul 2007

confirmed. We deposit Si_3N_4 layer with 140 nm thickness as an etching mask by plasma enhanced chemical vapor deposition (PECVD) process. Then a polymethylmethacrylate (PMMA) electron-beam resist layer is spin-coated on Si_3N_4 layer, and the PC CD2 microcavity patterns are defined by electron-beam (e-beam) lithography technology. After developing and fixing, the patterns are transferred into Si_3N_4 layer and MQWs by inductively coupled plasma/reactive ion etching (ICP/RIE) system. The Si_3N_4 hard mask is etched by CHF_3/O_2 mixed gas in RIE mode, and then $CH_4/Cl_2/H_2$ mixed gas is used to further transfer the patterns into MQWs at 150°C in ICP etching mode. Finally, a suspended membrane structure is formed by HCl selective wet etching. The top view and tilted view scanning-electron-microscope (SEM) pictures of fabricated high quality PC CD2 microcavity are shown in Figs. 4(a) and 4(b). The fabricated lattice constant and *r/a* ratio are 500 nm and ~0.33 in Fig. 4(a).

4. Lasing characterizations

The fabricated PC CD2 microcavities are optically pulse-pumped at room temperature by an 845 nm laser diode with 25 ns pulse width and 0.5% duty cycle. The light emitted from the microcavity is collected by a fiber and detected by an optical spectrum analyzer (OSA). The typical light-in light-out curve (L-L curve) of PC CD2 microcavity with a = 500 nm and r/a ratio ~ 0.33 is shown in Fig. 5(a) and the threshold can be estimated as 0.24 mW. The typical lasing spectrum at wavelength (λ) 1535.7 nm is shown in Fig. 5(b). We also show the spectrum near 0.9 times threshold in the upper inset of Fig. 5(a) and its linewidth ($\Delta\lambda_{FWHM}$) is 0.2 nm. The measured *Q*-factor can be estimated as 7700 by $\lambda / \Delta\lambda_{FWHM}$ in experiments [17]. It's worthy to note that the threshold and measured *Q*-factor are both worse than those of 12-fold QPC D2 microcavity with almost the same cavity modal boundary we reported before [10]. For high-symmetry (twelve) WGM resonance, this can be attributed to the non-uniform PBG confinement of triangular PCs with lower symmetry (six) level in *k*-space. Besides, the side-mode suppression-ratio (SMSR) of 18dB is estimated from the lower inset in Fig. 5(a). In our previous work [9], we proposed a simple approach to increase SMSR by inserting a central air hole in the cavity to destroy other resonance modes (in previous case, a dipole mode) without affecting WGM. However, this approach cannot be applied here because the main side mode observed in longer wavelength in Fig. 3(a) and Fig. 5(a) is also a WGM (K = 5). For mode identification, to confirm the lasing mode is WGM, we widen the slit of the OSA to collect the weak radiations from other resonance modes of the microcavity. The measured lasing spectrum in decibel scale is shown in Fig. 3(b). Comparing it with the 3D FDTD simulation results in Fig. 3(a), we obtain a very good match and clearly identify the lasing mode as WGM. Almost all resonance modes are observed and identified except for WGM (K = 7) near the gain region edge of MQWs. Besides, measured lasing results with a = 490-510

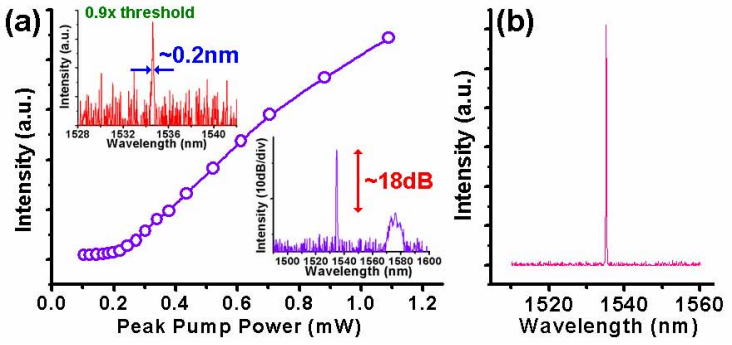

Fig. 5. (a). Typical L-L curve of PC CD2 microcavity laser. The threshold can be estimated as 0.24 mW from the curve. The upper inset also shows the spectrum near threshold and the measured *Q*-factor can be estimated as 7700 from the linewidth of 0.2 nm. The SMSR is also estimated as 18dB from the lower inset. (b) Typical lasing spectrum at 1535.7 nm.

#83638 - $15.00 USD Received 31 May 2007; revised 12 Jul 2007; accepted 12 Jul 2007; published 16 Jul 2007

nm and *r/a* ratio = 0.32-0.36 are also obtained and denoted by hollow circles, squares, and triangles (different shapes mean different lattice constants) in Fig. 3(a), which also quite match with the simulated results. The slight normalized frequency differences between measured and simulated results are arisen from the fabrication imperfections and the dimension estimation errors from SEM pictures.

5. Uniform cavity-waveguide coupling property

The PC-based cavity-waveguide structure [20, 21] is an important basic building block for various applications in PICs, such as optical interconnectors, couplers, optical buffers, and so on. Moreover, it is also a critical approach to convert most present PC microcavity lasers with vertical emissions to in-plane emissions in planar PICs. One of the key issues is the efficient coupling between the cavity and the waveguide. For efficient coupling, not only the mode frequencies but also the spatial mode distributions of cavity and waveguide should match with each other. A. Faraon *et al* [18] have investigated high coupling efficiency between high-*Q* PC L3 microcavity and PC single-defect waveguide. However, the coupling efficiencies are

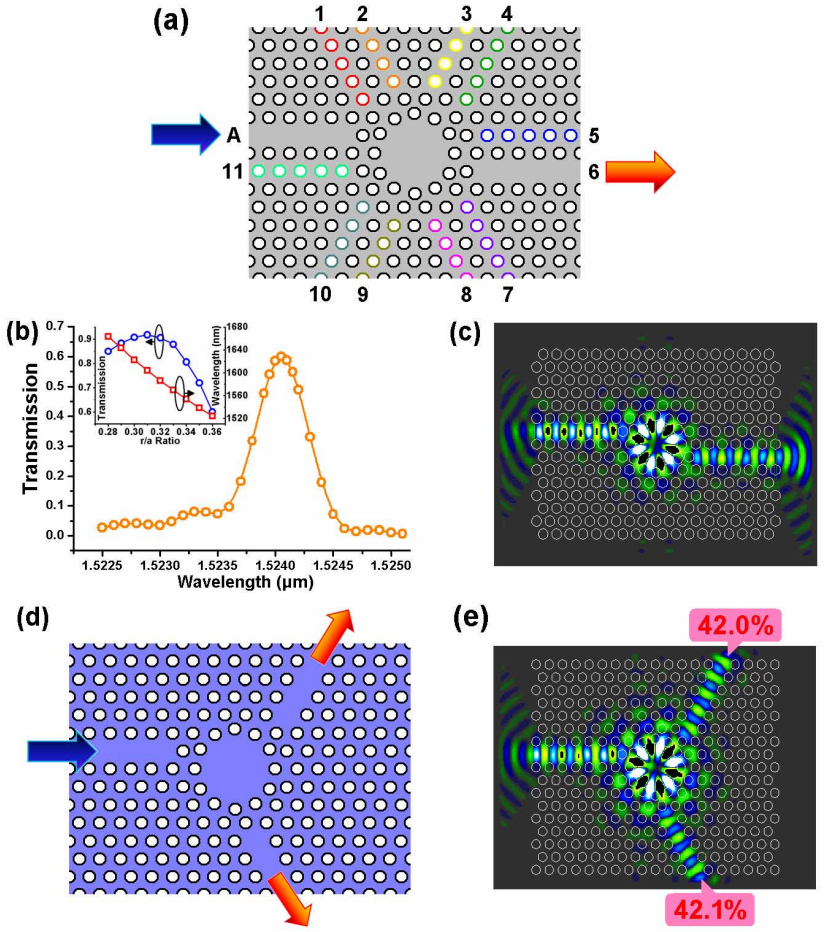

Fig. 6. (a). Scheme of waveguide-cavity-waveguide coupling system based on PC CD2 microcavity with different waveguide geometries. (Different output ports, numbered as port 1-10) (b) Transmission spectrum and (c) propagating field distribution of A-6 type coupler with *r/a* ratio of 0.36. The transmission is over 60%. The inset in (b) also shows the optimization of transmission versus *r/a* ratio. The maximum transmission appears when *r/a* ratio is equal to 0.31. (d) Scheme of A-4-8 coupler with power splitter function and (e) its propagating field distribution. The output powers of port 4 and port 8 are almost the same with 42% transmission.

#83638 - $15.00 USD Received 31 May 2007; revised 12 Jul 2007; accepted 12 Jul 2007; published 16 Jul 2007

not uniform in different directions due to the specific resonance direction of the mode. This would be an un-neglected problem under some specific designs where multiple output ports are needed. Based on PC CD2 microcavity, we propose our initiative design to solve this problem. It can be found that the evanescent field of each lobe of WGM propagates along 12 different directions from the microcavity as shown in Fig. 2(c). Instinctively, because every lobe of WGM is identical to each other, uniform coupling efficiencies can be obtained between the cavity and the inserted PC waveguides along these directions. To investigate this uniform coupling behavior, we first numerically study the transmission of waveguide-cavity-waveguide structure in 180° line-to-line geometry (labeled as A-6 type) as shown in Fig. 6(a) by two-dimensional (2D) FDTD method with approximated index 2.7. The separation between the cavity and waveguide is properly chosen as two lattice periods. Under the parameters of a = 500 nm and r/a ratio = 0.36, the detected transmission from the output port is around 60%. The transmission is defined as the ratio of the detected powers 5 lattice-period distance after and before the microcavity. The transmission spectrum and field distribution with significant WGM resonance are shown in Figs. 6(b) and 6(c). The transmission is also optimized by varying r/a ratio from 0.28 to 0.36. The highest transmission is over 90% when r/a ratio = 0.30-0.32, as shown in the inset of Fig. 6(b). Also, the propagation loss caused by the PC waveguide has been considered and normalized. To initiatively confirm the uniform coupling characteristic in different propagating directions corresponding to each WGM lobe, we calculate the transmissions of geometries with the same input A but different output ports numbered 1 to 10 as denoted and shown in Fig. 6(a). The r/a ratio is set as 0.32 according to the optimization result. The simulated transmissions and wavelengths of different geometries are listed in Table 1. In Table 1, the transmissions are found to be in the range of 91%-93%, which indicates the uniform coupling in different propagation directions, i.e. uniform coupling in different waveguide-cavity-waveguide geometries. We also calculate the transmission of aninserted output waveguide between ports 5 and 6 for comparison, and we find that for WGM (K = 6), the transmission dramatically decreases to lower than 2%. It is necessary to notice that we do not consider A-11 type because this geometry will involve additional coupling effects for the wave propagation in the parallel waveguides [19] and make the analysis more complicated. We also design a coupler with one input port A and two output ports 4 and 8 named A-4-8 type under proper choice as shown in Fig. 6(d). Almost the same

Table 1. Transmissions and wavelengths of different waveguide-cavity-waveguide geometries named A-1 type to A-10 type.

Type	Transmission	Wavelength	Type	Transmission	Wavelength
A-1	91.9%	1586.4nm	**A-6**	90.9%	1586.2nm
A-2	91.5%	1586.3nm	**A-7**	92.9%	1586.3nm
A-3	91.9%	1586.3nm	**A-8**	91.3%	1586.3nm
A-4	92.5%	1586.3nm	**A-9**	91.8%	1586.3nm
A-5	93.0%	1586.3nm	**A-10**	92.9%	1586.3nm

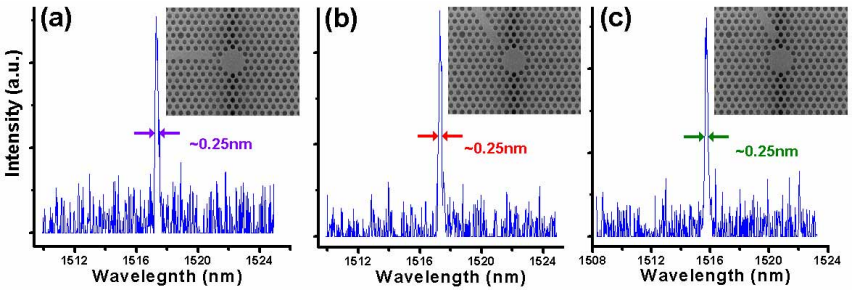

Fig. 7. (a)-(c) SEM pictures and measured lasing spectra near threshold of PC CD2 microcavities with inserted waveguides along three different directions. The measured linewidths all degrade to 0.25 nm.

#83638 - $15.00 USD Received 31 May 2007; revised 12 Jul 2007; accepted 12 Jul 2007; published 16 Jul 2007

transmission ~ 42% in each output port is achieved as shown in Fig. 6(e). This indicates that PC CD2 microcavity with WGM combined with PC waveguide is very suitable in designing PC-based components that need multi-port functions.

To investigate this uniform coupling property in experiments, we fabricate PC CD2 microcavities with waveguides along three different directions. The SEM pictures and lasing spectra near threshold are shown in Figs. 7(a)-7(c). The measured *Q*-factors degrade to around 6100 from the measured linewidth (~ 0.25 nm) near 0.9 times threshold for all three cases. This uniform degradation also indicates the uniform coupling behavior in different cavity-waveguide geometries. We believe this PC CD2 microcavity would be very potential in designing and realizing PC-based active source in planar PICs, photonic molecule, optical interconnector, coupled-resonator optical waveguide (CROW), and so on. Besides, this microcavity provides us more flexibility and freedom in designing various waveguide-cavity-waveguide geometries for above applications due to its uniform coupling property.

6. Conclusion

In summary, based on the concept of cavity-shaping in micro-disk and micro-gear lasers, we have proposed a PC circular-shaped D2 microcavity with periodic gears formed on the cavity edge by shifting the 12 nearest air holes to be circular arrangement with one lattice constant spacing. The modal characteristics of WGM with azimuthal number six are numerically simulated by 3D FDTD method. From well-fabricated devices, we obtain single-mode lasing action with low threshold of 0.24 mW, high measured *Q*-factor of 7700, and SMSR of 18dB. By comparing with the 3D FDTD simulated results, we confirm and identify the lasing mode as WGM (K = 6). Based on this microcavity design, we also initiatively demonstrate the uniform coupling property between the cavity and the inserted waveguides in different directions by calculating their transmissions (91%-93%) in FDTD simulations and measuring the *Q*-factor degradations in experiments. This uniform coupling property provides more flexibility in designing waveguide-cavity-waveguide structures in planar PIC applications, especially for those that need multiple output ports.

Acknowledgments

This work is supported by Taiwan's National Science Council (NSC) under contract numbers NSC-95-2221-E-009-234 and NSC-95-2221-E-009-056, Promoting Academic Excellence of Universities under contract number NSC-96-2752-E-009-007-PAE. The authors would like to thank the help from Center for Nano Science and Technology (CNST) of National Chiao Tung University, Taiwan.

#83638 - $15.00 USD Received 31 May 2007; revised 12 Jul 2007; accepted 12 Jul 2007; published 16 Jul 2007